This article has not been copyedited and formatted. The final version may differ from this version.
DMD Fast Forward. Published on September 19, 2007 as doi:10.1124/dmd.107.016055

DMD #16055

IN VITRO METABOLISM OF THE ANALGESIC BICIFADINE IN THE MOUSE, RAT, MONKEY, AND HUMAN

David A. Erickson, Stacy Hollfelder, Justin Tenge, Mark Gohdes, Jeffrey J. Burkhardt,

and

Philip A. Krieter

Department of Drug Metabolism, Covance Laboratories Inc., Madison, Wisconsin

(D.A.E., S.H.,J.T., M.G., J.B.) and DOV Pharmaceutical Inc, Somerset, NJ (P.A.K.)

DMD Fast Forward. Published on September 19, 2007 as DOI: 10.1124/dmd.107.016055
This article has not been copyedited and formatted. The final version may differ from this version.

Running Title: *In vitro* Metabolism of [^{14}C]Bicifadine

Corresponding Author: Philip A. Krieter, Ph.D.

DOV Pharmaceutical, Inc.

150 Pierce Street

Somerset, NJ 08873

Phone: 732-907-3658

Fax: 732-907-2797

e-mail: pkrieter@dovpharm.com

Number of text pages: 27

Number of tables: 4

Number of figures: 9

Number of references: 24

Number of words in Abstract: 199

Number of words in Introduction: 256

Number of words in Discussion: 1034

Abbreviations:

amu, atomic mass unit; AO, aldehyde oxidase; cDNA, recombinant DNA; CYP, cytochrome P450; EDTA, ethylenediamine tetraacetic acid; HPLC, high performance liquid chromatography; Km, concentration at one-half of maximum velocity; LC, liquid chromatography; LC/MS, liquid chromatography/mass spectrometry; LC/MS/MS, liquid chromatography-tandem mass spectrometry; MAO, monoamine oxidase; *m/z*, mass to

DMD Fast Forward. Published on September 19, 2007 as DOI: 10.1124/dmd.107.016055
This article has not been copyedited and formatted. The final version may differ from this version.

charge ratio; MS, mass spectrometer; RO, reverse osmosis; R_t, retention time; UGT, uridine diphosphoglucuronic acid transferase; V_{max}, maximum velocity; v/v, volume to volume; DOV 220,075, bicifadine, [(±)-1-(4-methylphenyl)-3-azabiocyclo[3.1.0]hexane hydrochloride.

DMD Fast Forward. Published on September 19, 2007 as DOI: 10.1124/dmd.107.016055
This article has not been copyedited and formatted. The final version may differ from this version.

ABSTRACT

The *in vitro* metabolism of [^{14}C]bicifadine by hepatic microsomes and hepatocytes from mouse, rat, monkey, and human was compared using radiometric HPLC and LC/MS/MS. Two main metabolic pathways were identified in all four species. One was an NADPH-dependent pathway in which the methyl group was oxidized to form a hydroxymethyl metabolite (M2). Its formation was inhibited in human microsomes only by quinidine, a CYP2D6 inhibitor. In incubations with individual cDNA-expressed human CYPs, M2 was formed only by CYP2D6 and CYP1A2, with CYP2D6 activity 6-fold greater than that of CYP1A2. M2 was oxidized further to the carboxylic acid metabolite (M3) by hepatocytes from all four species. The second major metabolic pathway was an NADPH-independent oxidation at the C-2 position of the pyrrolidine ring, forming a lactam metabolite (M12). This reaction was almost completely inhibited in human hepatic microsomes and mitochondria by the MAO-B specific inhibitor selegiline. Clorgyline, a specific inhibitor of MAO-A, was less effective in inhibiting M12 formation. Other metabolic pathways of variable significance among the four species included the formation of carbamoyl-O-glucuronide, hydroxymethyl lactam, and carboxyl lactam. Overall, the data indicate that the primary enzymes responsible for the primary metabolism of bicifadine in humans are MAO-B and CYP2D6.

DMD Fast Forward. Published on September 19, 2007 as DOI: 10.1124/dmd.107.016055
This article has not been copyedited and formatted. The final version may differ from this version.

Bicifadine [(±)-1-(4-methylphenyl)-3-azabiocyclo[3.1.0]hexane hydrochloride; DOV 220,075 HCl, Figure 1], an inhibitor of norepinephrine and serotonin uptake, is being developed for the treatment of acute and chronic pain. Bicifadine is a non-narcotic analgesic (Epstein et al., 1982) that is active in models of neuropathic pain with no evidence of abuse liability potential (Basile et al., 2007). Clinically, it has been shown to be effective in the treatment of acute dental pain (Stern et al., 2005) and bunionectomy pain (Riff et al., 2006). Bicifadine was also reported to be as effective as the standard of care in reducing chronic lower back pain (Stern et al., 2006).

In order to interpret the significance of preclinical and toxicological investigations to humans, it is important to understand the metabolism of bicifadine and demonstrate that the toxicology species are exposed to the same metabolites that occur in humans. Consequently, *in vitro* metabolism studies using hepatic microsomes and hepatocytes from mice, rats, monkeys, and humans were conducted using [^{14}C]bicifadine. The metabolic profiles of [^{14}C]bicifadine were compared in the four species using hepatic microsomes and hepatocytes. Additionally, the principal enzymes responsible for the metabolism of [^{14}C]bicifadine were identified to determine the potential for bicifadine to be involved in drug-drug interactions.

During the course of the investigations, evidence was generated demonstrating that the formation of the main metabolite, a lactam, involved the action of a MAO, primarily MAO-B. Data are presented demonstrating that liver microsomes, in addition to mitochondria, have a high capacity for this reaction.

Materials and Methods

Chemicals. [^{14}C]Bicifadine (44 mCi/mmol; 254 μCi/mg) was supplied by Vitrax Company (Placentia, CA); its radiochemical purity was >99% by HPLC. A reference standard of bicifadine was supplied by DOV Pharmaceutical. Clorgyline, selegiline, phthalazine, phthalazinone, and perphenazine were obtained from Sigma-Aldrich Chemical Co. (St. Louis, MO). All other chemicals and solvents were obtained from commercial sources and were of the highest quality available.

Enzyme Preparations. Hepatic microsomes from male CD-1 mice, male Sprague Dawley rats, and male cynomolgus monkeys were obtained from BD Biosciences (Woburn, MA). Pooled hepatic microsomes from male and female humans were obtained from CellzDirect (Pittsboro, NC) or from Tissue Transformation Technologies (Edison, NJ). Pooled human liver mitochondria from three male and three female donors were obtained from XenoTech, LLC (Lenexa, KS). Isolated fresh primary hepatocytes from male mouse, male rat, male monkey, and human were supplied by CellzDirect. The human donor was a 54-year old non-smoking female with no known history of exposure to hepatitis B or C or HIV. Recombinant (cDNA-expressed) human cytochromes P450, MAO-A, and MAO-B (Supersomes™, microsomes prepared from baculovirus-infected BTI-TN-5B1-4 insect cells) were obtained from BD Gentest Corporation (Woburn, MA).

Incubations. *Microsomal CYP activity.* Hepatic microsomal incubations were performed in 100 mM phosphate buffer containing 1 mM EDTA and 3 mM $MgCl_2$ (pH 7.4) at a final assay volume of 1 ml and microsomal protein concentration of

DMD Fast Forward. Published on September 19, 2007 as DOI: 10.1124/dmd.107.016055
This article has not been copyedited and formatted. The final version may differ from this version.

0.25 mg/ml. Incubations were performed at 37°C and contained 1 mM NADPH and 10 μM bicifadine. Bicifadine and [^{14}C]bicifadine were combined to maintain radioactivity levels at approximately 1 x 10^6 dpm/ml. Incubations were initiated by the addition of 10 μl of a 100-fold concentrated solution of [^{14}C]bicifadine. Incubations were terminated at 0, 5, 10, 20, and 30 min by the addition of 2 ml ice-cold acetonitrile. Control incubations were performed as above at 0 and 30 min in the absence of NADPH. Heat-inactivated microsomes were prepared by heating in boiling water for 10 min. Terminated incubation samples were mixed and the protein removed by centrifugation at 1400*g* for 10 min at 4°C. The supernatants were stored at approximately -20°C until analysis. When appropriate, CYP-specific inhibitors were added at the following concentrations: 10 μM α-naphthoflavone (CYP1A2), 5 μM sulfaphenazole (CYP2C9), 25 μM omeprazole (CYP2C19), 10 μM quinidine (CYP2D6), 100 μM DETC (CYP2E1), and 1 μM ketoconazole (CYP3A4). Similar assay conditions were used for cDNA-expressed CYPs except that they were used at a final assay concentration of 50 pmol CYP/mL with an incubation time of 30 min only. Vector control samples testing for inherent CYP metabolic activity were performed in the presence and absence of NADPH with Supersomes™ prepared from insect cells (BTI-TN-5B1-4) treated with vector only (no cDNA). Control incubations were performed in the presence and absence of NADPH with each set of control Supersomes™ for 30 min. CYP2A6 and CYP2C9 were run in TRIS buffer per manufacturer's recommendations. Vector controls for these isozymes were also run with TRIS buffer.

MAO Assay in Mitochondria/Microsomes. Incubations were performed as above with the following modifications. The final protein concentrations in the assays were

0.5 mg/ml for microsomes, 1.0 mg/ml for mitochondria, or 1.0 mg/ml for cDNA expressed MAO-A and MAO-B. When appropriate, 1 to 1000 nM (final concentrations) of clorgyline or selegiline were added to incubations and were incubated for 20 min prior to the addition of a 100-fold concentrated solution of [^{14}C]bicifadine.

Aldehyde Oxidase (AO) Assay in Mitochondria/Microsomes/Cytosol. Incubations were performed as above with the following modifications. The final protein concentration in the assay using cytosol was 1 mg/ml. When appropriate, 1 µM (final concentration) of perphenazine was added to incubations and was incubated for 15 min prior to the addition of a 100-fold concentrated solution of [^{14}C]bicifadine (1 µM final concentration) or phthalazine (10 µM final concentration). Analytical conditions for phthalazine oxidase were as described by Obach (2004).

Hepatocytes. The gels containing the fresh hepatocyte suspensions were reconstituted per supplier's recommendations into William's E medium at a hepatocyte density of approximately 0.75 x 10^6 cells/ml. Hepatocyte viability, based on trypan blue exclusion, was 85.5, 87.0, 89.8, and 73.8% for mouse, rat, monkey, and human hepatocytes, respectively. Metabolic capacity of hepatocytes was assessed throughout the 180-min incubation period by monitoring their ability to metabolize 7-ethoxycoumarin. CYP, UGT, and sulfotransferase activities were active over 180 min for all four species. The cells were preincubated for 30 min in an incubator set to maintain 37°C in an atmosphere of 5% CO_2 in air. Reactions were initiated by adding 10 µl of the appropriate [^{14}C]bicifadine fortification solution. Incubations were terminated at 0, 60, and 180 min by adding 2 ml acetonitrile. For the time 0 incubations, the hepatocyte suspension was cooled on ice for 10 min, 10 µl of the appropriate

DMD Fast Forward. Published on September 19, 2007 as DOI: 10.1124/dmd.107.016055
This article has not been copyedited and formatted. The final version may differ from this version.

fortification solution was added, and then 2 ml acetonitrile was added. Terminated incubation samples were vortex mixed and the protein removed by centrifugation at 1400*g* for 10 min at 4°C. The supernatants were stored at -20°C until analysis. Control incubations were conducted at all time points by incubating the appropriate concentrations of [^{14}C]bicifadine in William's E medium in the absence of hepatocytes.

HPLC Analysis. Acetonitrile extracts from microsomal or hepatocyte incubations were mixed, concentrated to dryness using a stream of nitrogen, and reconstituted with 500 µl of 0.1% formic acid:acetonitrile (9:1, v:v). The samples were then mixed, sonicated for 20-25 min, and analyzed by HPLC. Analysis was performed on an Alltech® Prevail™ C_{18} column (4.6 x 150 mm, 5-µm particle size, Alltech Associates, Inc, Deerfield IL) preceded by a Phenomenex® SecurityGuard™ C_{18} guard column (4 x 3 mm, Phenomenex Inc, Torrance CA). The column was interfaced with a Packard Series A-500 radioactivity detector (Perkin-Elmer, Meriden CT) equipped with a 0.5 ml TRLSC flow cell. The liquid scintillation flow rate was 3 ml Ultima Flo™ M/min. For most experiments, mobile phase A was 0.05% formic acid in water, mobile phase B was acetonitrile, and the flow rate was 1 ml/min. For metabolite identification, the initial mobile phase of 97:3 A:B was increased linearly to 90:10 A:B from 5 to 7 min and held constant until 25 min. The mobile phase was then increased linearly to 5:95 A:B from 25 to 36 min; after another 9 min, it was re-equilibrated to 97:3 A:B. For experiments using CYP inhibitors and cDNA-expressed enzymes, the initial gradient was 95:5 A:B; after 2 min, it was increased linearly to 50:50 A:B at 25 min. The mobile phase was increased to 10:90 A:B to remove any residual material and then re-equilibrated to 95:5 A:B.

LC/MS/MS Analysis. For metabolite identification, the LC/MS/MS studies were conducted using a Shimadzu LC system controller and pumps (Models SCL-10A VP and LC-10AD VP, respectively). A Phenomenex® Luna® C18 HPLC column was used with the same mobile phases A and B and acetonitrile gradient as used for metabolite separation described above. After passing through a column switcher, the HPLC column effluent was split with approximately 30% of the flow diverted to the mass spectrometer (Micromass Quattro II with an ESP Z-Spray source in the positive ion mode) and 70% to the radiometric detector (2.1 ml Packard Ultima-Flo M LSC cocktail/min). MS settings were as follows: cone voltage, 10 to 28 V; mass range, 40 to 600 amu; scan time, 0 to 40-45 min; source block temperature, 130ºC; desolvation temperature, 300ºC; ESI nebulizer gas, 15 l/hr (N_2); bath gas, 400 l/hr (N_2). The product ion LC/MS/MS analyses used the same instrumentation and conditions as for the full-scan LC/MS analyses with the following exceptions to the MS conditions: cone voltage, 22 V; collision energy, 15-24 eV; collision gas, argon.

For the CYP reaction phenotyping experiments with bicifadine lactam, analyses were performed using a Shimadzu LC system controller and pumps (Models SIL-HTc and LC-10AD VP, respectively). The HPLC columns, mobile phases, and acetonitrile gradient were the same as used for metabolite separation described above. After passing through a column switcher, the HPLC column effluent was split with approximately 30% of the flow diverted to the mass spectrometer (Micromass Quattro II with an ESP Z-Spray source in the positive ion mode) and 70% to the radiometric detector (2.1 ml Packard Ultima-Flo M LSC cocktail/min). MS settings were as follows: cone voltage, 10 to 28 V; mass range, 40 to 600 amu; scan time, 0 to 40-45 min; source

DMD Fast Forward. Published on September 19, 2007 as DOI: 10.1124/dmd.107.016055
This article has not been copyedited and formatted. The final version may differ from this version.

block temperature, 130ºC; desolvation temperature, 300ºC; ESI nebulizer gas, 15 l/h (N_2); bath gas, 400 l/h (N_2).

RESULTS

Comparative Metabolism of [^{14}C]Bicifadine. [^{14}C]Bicifadine was incubated with hepatic microsomes and hepatocytes from mouse, rat, monkey, and human. There were 16 radiolabeled peaks other than [^{14}C]bicifadine that were observed among the incubations. Discrete metabolic peaks are labeled on radiochromatograms according to their order of elution. Representative radiochromatograms displaying metabolite profiles for the microsomes and hepatocytes are presented in Figures 2 and 3, respectively, and the percentages of total radioactivity attributed to each of the metabolites are listed in Table 1 and 2. Due to the high specific activity of the [^{14}C] used in the experiments, the protonated molecular ion and the radiolabel-containing product ions were two amu higher than that of the nonradioactive compound.

A potential metabolite (M13), constituting 4 to 14% of the profiled radioactivity among the incubations, was present in approximately equal amounts at 0 and 30 min of incubation. Based on LC/MS/MS analysis (*m/z* 204 of protonated molecular ion), it was putatively identified as N-formyl [^{14}C]bicifadine. Since formic acid was a constituent of the sample resuspension solution and M13 formation was time- and NADPH-independent, it was considered to be an artifact formed during sample preparation.

Microsomes. In hepatic microsomal incubations, two principal metabolites of [^{14}C]bicifadine were detected among the four species, M2 and M12. A major metabolite from all four species, M12, was identified as [^{14}C]bicifadine lactam, formed by oxidation at the 2-position of the pyrrolidine ring. It constituted approximately 5 to 8% of the profiled radioactivity in rat and human microsomes, 18% in mouse microsomes, and 36% in monkey microsomes (Table 1). The formation of M12 did not require the

presence of NADPH and it formed equally well in incubations with or without NADPH. It had a protonated molecular ion at *m/z* 190, 14 amu higher than that of [^{14}C]bicifadine (Table 3, Figure 4B). The product ion mass spectrum for *m/z* 190 gave ions at *m/z* 173 (-NH_3), 172 (-H_2O), 143, 134, 105, 98, and 57. The ion at *m/z* 105 indicated that the toluene moiety was not modified while the ions at *m/z* 57 and 134 indicated that an oxidation had occurred at the 2-position of the pyrrolidine ring. [^{14}C]M9 had the same product mass spectrum as an authentic standard of the compound (DOV 255,833), with the exception of the ions that were 2 amu higher due to the presence of the [^{14}C] atom with a high specific activity (Data Supplement Figure 2). The second principal metabolite, M2, was approximately as abundant as M12 in rat and human and was identified as hydroxymethyl [^{14}C]bicifadine. Its formation was NADPH-dependent. M2 had a protonated molecular ion at *m/z* 192, 16 amu higher than that of [^{14}C]bicifadine. The product ion mass spectrum for *m/z* 192 gave ions at m/z 175 (-NH_3), 162, 157, 149 (-C_3H_3N), 145 (*m/z* 175 -C_2H_6), 130, and 121 (*m/z* 149 - C_2H_4). The presence of the ions at *m/z* 149 and 121 indicated that hydroxylation had occurred on the methyl group.

Other metabolites detected in radiochromatograms from microsomal incubations were M3 and M8. M3 was identified as carboxyl [^{14}C]bicifadine and was present in hepatic microsomal incubations from all four species, although in human it was detectable by LC/MS only. The protonated molecular ion of M3 was at *m/z* 206, 30 amu higher than [^{14}C]bicifadine. The product ion mass spectrum for *m/z* 206 gave ions at *m/z* 189 (-NH_3), 171, 163 (-C_2H_3N), 145 (*m/z* 189 -CO_2), 135 (*m/z* 163 -C_2H_4), 130, 128, and 117. The ions at *m/z* 163 and 135 indicated that the methyl group had been oxidized to the carboxylic acid. M8 was identified as hydroxymethyl [^{14}C]bicifadine

lactam and was present in mouse and monkey incubations, although in mouse it was detectable by LC/MS only. The protonated molecular ion of M8 was at *m/z* 206, also 30 amu higher than [^{14}C]bicifadine. The product ion mass spectrum for *m/z* 206 gave ions at *m/z* 188 (-H_2O), 174, 159 (-$^{14}CH_3NO$), 150, 129, 121, 105, 93, 84, and 57. The ion at *m/z* 121 indicated that hydroxylation had occurred on the methyl group. The differences in the way that M8 fragmented with respect to [^{14}C]bicifadine indicated that a modification had occurred on the pyrrolidine ring. Specifically, ions at *m/z* 57 and 150 indicated that an oxidation had occurred at the 2-position of the pyrrolidine ring.

Three minor metabolites (MA, MB, and MC) were detected only in microsomal incubations in low amounts and their formation was neither time- nor NADPH-dependent. Their protonated molecular ions are *m/z* 190, *m/z* 299, and *m/z* 215 for MA, MB, and MC, respectively; their identities are uncertain.

Hepatocytes. In hepatocyte incubations using 10 µM [^{14}C]bicifadine, the principal metabolites, depending on the species, were M2, M3, M9, and M12. In all species, unchanged [^{14}C]bicifadine was a minor component after 180 min of incubation (Figure 3).

In mice, two of the main metabolites were M3 and M12. The other major metabolite, M9, was the lactam acid of [^{14}C]bicifadine. Its protonated molecular ion was at *m/z* 220, 44 amu higher than that of [^{14}C]bicifadine. The product ion mass spectrum for *m/z* 220 gave ions at *m/z* 203 (-NH_3), 202 (-H_2O), 184, 173, 164, 159, 146, 135, 129, 117, 107, 98, 91, 85 and 57. The presence of the ion at *m/z* 135 indicated that the methyl group had been oxidized to a carboxylic acid. Similar to M8, the fragmentation of M9 indicated that an oxidation had occurred at the 2-position of the pyrrolidine ring.

The product mass spectrum of an authentic standard of M12 (DOV 255,828) had the same fragmentation as [^{14}C]M12 with the exception of the ions due to the presence of the radiocarbon atom, which increased the amu by 2 (Data Supplement Figure 3).

In rat hepatocyte incubations, the major metabolite was M12 with lesser percentages of M3 and M9. Two minor metabolites, M5 and M6, had very similar mass spectra. Based on their protonated molecular ion (*m/z* 262) and fragmentation, both structures were deduced to be N-acetylated M9. The difference in their retention times may be due to the position of the acetyl group relative to the plane of the pyrrolidine ring. The immediate precursor to M5 and M6 could not be determined based on the present results.

The major metabolites in monkey hepatocytes were M9, M3, and M2. Also detected as significant metabolites in monkey hepatocytes were M8 and its O-glucuronide conjugate (M7). A glutathione adduct of [^{14}C]bicifadine (M4) was detected only in incubations from monkey hepatocytes. The protonated molecular ion was at *m/z* 481, 305 amu higher than that of [^{14}C]bicifadine; the specific site of attachment could not be determined.

In humans, the major metabolite was M12 with lesser amounts of M3. As in the rat, human hepatocytes produced a small amount of M10, with a protonated molecular ion of *m/z* 192, 16 amu higher than that of [^{14}C]bicifadine. The presence of the ions at *m/z* 105 and 91 indicated that the hydroxylation had not occurred on the toluene group while ions at *m/z* 59 and 134 indicated that oxidation had occurred at the C2 position of the pyrrolidine ring.

DMD Fast Forward. Published on September 19, 2007 as DOI: 10.1124/dmd.107.016055
This article has not been copyedited and formatted. The final version may differ from this version.

All four incubations produced limited amounts of the carbamoyl O-glucuronide of [^{14}C]bicifadine (M11). Its protonated molecular ion was 220 amu higher than that of the parent compound and had a number of similarities with that of [^{14}C]bicifadine (*m/z* 159, 144, and 105). The loss of 176 amu from the protonated molecular ion to produce the ion at m/z 220 indicated that M11 was a glucuronide conjugate.

The proposed metabolic scheme for [^{14}C]bicifadine is presented in Figure 5.

Reaction phenotyping of [^{14}C]bicifadine metabolism in human. When 1 μM [^{14}C]bicifadine was incubated with pooled human liver microsomes, M2 (R_t = 8.0 min) and M12 (R_t = 23.9 min) were the main metabolites formed (Fig 6). Their identities were confirmed by LC/MS/MS. The absence of NADPH in the incubation mixture did not change the rate of formation of M12 and neither metabolite was formed by heat-deactivated microsomes (data not shown).

In order to determine which enzyme(s) were responsible for the formation of the NADPH-dependent metabolite M2, experiments were performed utilizing pooled microsomes with CYP-selective inhibitors. Quinidine, a selective inhibitor of CYP2D6, was the only CYP450 inhibitor that decreased microsomal M2 formation rates (Figure 7). This observation was confirmed using cDNA-expressed isozymes. cDNA-Expressed CYP2D6 formed M2 at a rate of 0.053 pmol/min/pmol CYP. CYP1A2 also produced M2, but at a much lower rate (0.006 pmol/min/pmol CYP). No detectable formation of M2 was observed with cDNA-expressed CYP2A6, 2B6, 2C8, 2C9, 2C19, 2E1, or 3A4 (data not shown).

The oxidation of [^{14}C]bicifadine to M12 in the absence of NADPH indicated that this reaction was catalyzed by neither CYP nor flavin-containing monooxygenase.

Experiments were performed to investigate whether MAO could be involved in its formation. After preincubation of human liver microsomes with increasing concentrations of the MAO-B inhibitor selegiline, the formation of M12 declined by >90% from 37.7 pmol/min/mg protein to 2.35 pmol/min/mg (Table 4). In contrast, the MAO-A inhibitor clorgyline at concentrations up to 1 μM had only a modest effect on the rate of microsomal M12 formation.

Subsequently, the kinetics of M12 formation were determined in pooled human hepatic microsomal incubations containing increasing concentrations of [^{14}C]bicifadine (Figure 8). The data suggested biphasic kinetics, although it was not possible to accurately estimate the low affinity kinetic phase due to the range of concentrations tested. The high affinity phase had apparent K_m and V_{max} values of 3.72 μM and 129 pmol/min/mg protein while the values for the low affinity phase were 328 μM and 1390 pmol/min/mg protein. The intrinsic clearance values (V_{max}/K_m) for the high and low affinity enzymes were calculated to be 34.7 and 4.2 μL/min/mg protein, respectively.

MAO is considered to be present mainly in the mitochondrial fraction of the cell. Therefore, [^{14}C]bicifadine was incubated with pooled human mitochondria and increasing concentrations of the two MAO inhibitors. Similar to microsomal incubations, 1 μM clorgyline had little effect on the formation of M12 by mitochondria while 1 μM selegiline decreased mitochondrial M12 formation rates from 17.3 to 2.67 pmol/min/mg protein (Table 4). As a confirmation of this observation, [^{14}C]bicifadine was incubated with cDNA-expressed MAO-A and MAO-B and M12 was also formed at rates of 5.5 ± 1.1 and 2.6 ± 1.3 pmol/min/mg protein, respectively.

While the action of MAO normally results in the cleavage of the carbon-nitrogen bond, the oxidation of the neurotoxin MPTP by MAO-B has been shown to stop at the formation of an imine (Chiba et al., 1985). Further oxidation to the MPTP lactam is due to the cytosolic enzyme AO (Yoshihara and Ohta, 1998). In order to check for residual activity in the cell fractions, the AO substrate phthalazine was incubated with liver cytosol, microsomes, and mitochrondria in the presence and absence of 1 μM perphenazine, an AO inhibitor. Cytosolic AO was inhibited 55% (Figure 9), confirming the effectiveness of the inhibitor. Residual AO activity was also present in the microsomal and mitochondrial fractions and was inhibited 30 and 26%, respectively, by perphenazine. In contrast, the oxidation of [^{14}C]bicifadine to the lactam M12 was not affected by perphenazine, suggesting that AO is not involved in the formation of M12.

Although a minor metabolic pathway, CYP reaction phenotyping experiments were also conducted for the formation of M8 from M12. None of the CYP-specific inhibitors were particularly effective against M8 formation. However, some degree of inhibition was observed with α-naphthoflavone (30% inhibition, selective for CYP1A2), sulfaphenazole (9% inhibition, selective for CYP2C9), omeprazole (13% inhibition, selective for CYP2C19) and diethyldithiocarbamate (14% inhibition, selective for CYP2E1). When M12 was incubated with a battery of cDNA-expressed CYPs, M8 was formed to some extent by all of the enzymes examined except CYP2A6. However, the enzymes that most efficiently formed M8 were CYP2C19 (1.27 pmol/min/pmol CYP), CYP1A2 (0.969 pmol/min/pmol CYP), CYP2D6 (0.717 pmol/min/pmol CYP), and CYP2E1 (0.367 pmol/min/pmol CYP).

DISCUSSION

The major metabolic pathways of [^{14}C]bicifadine were similar among the four species examined when the results using hepatic microsomes and isolated hepatocytes were compared. One of the two major metabolic pathways is initiated by hydroxylation of the methyl group to form M2. In human microsomes, this reaction is catalyzed predominantly by CYP2D6 with minor involvement of CYP1A2. M2 is oxidized further in hepatocytes from all four species to the carboxylic acid metabolite M3. Based on the combined percentages of M2 and M3, approximately 15% of [^{14}C]bicifadine is metabolized via this pathway in rat and human hepatocytes while 42% is metabolized by this pathway in the monkey. A clinical trial would be needed to determine if concomitant administration of CYP2D6 inhibitors could affect the clearance of bicifadine.

Like bicifadine, M12 is also oxidized to a hydroxymethyl metabolite (M8). Thus, it was of interest to determine whether this reaction was also carried out by CYP2D6. A variety of cDNA-expressed human CYPs were capable of producing this metabolite, including CYP2D6. However, quinidine (selective for CYP2D6) was ineffective as an inhibitor of M8 formation in microsomal incubations, indicating that CYP2D6 is not involved in this reaction. Although CYP2D6 may have a limited capacity for M8 formation from M12, the enzymes primarily responsible for this reaction appear to be CYP1A2, CYP2C19, and CYP2E1.

The other major pathway for the metabolism of [^{14}C]bicifadine is oxidation of the C2 carbon of the pyrrolidine ring to form the lactam metabolite M12. Approximately equal amounts were formed by microsomes in the presence and absence of NADPH

from all four species, indicating that the oxidation was not due to either CYP450 or flavin-containing monooxygenase. The reaction is catalyzed mainly by MAO-B as determined by the addition of the specific inhibitor selegiline to incubations with microsomes and mitochondria. Formation of M12 declined by 94% in the presence of 1 μM selegiline when compared to control incubations. MAO-A may be involved to a lesser extent since the formation of M12 declined approximately 11% when 1 μM clorgyline was added to the microsomal suspensions.

Lactam formation from an aliphatic carbon-nitrogen bond has been shown to be due to the sequential action of MAO-B (Chiba et al., 1985), or CYP450 (Cashman et al., 1992), followed by oxidation of the resulting imine by cytosolic AO (Yoshihara and Ohta, 1998; Brandlange and Lindblom, 1979; Vickers and Polsky, 2000). The presence of residual AO activity in the microsomal and mitochondrial fractions precludes eliminating this enzyme's involvement in the formation of M12. But the addition of the AO inhibitor perphenazine to the incubations had no effect on the oxidation of bicifadine to M12. Also, AO oxidizes quaternary azaheterocyclic imines to lactams but has little to no activity on tertiary azaheterocyclic imines (Beedham, 2002). The putative intermediate imine of bicifadine formed by MAO-B would have a tertiary structure. While the present findings indicate that MAO is critical to the formation of the bicifadine lactam M12, the identification of the enzyme that catalyzes the oxidation of the putative imine intermediate to the lactam requires further investigation.

The inhibition of M12 formation in hepatic microsomes by MAO-B inhibitors was unexpected since this is considered a mitochondrial enzyme (Schnaitman et al, 1967). MPTP is oxidized to $MPDP^+$ predominantly by mitochondrial MAO-B; the microsomal

fraction produced mainly the N-desmethyl and N-oxide metabolites but very little $MPDP^+$ (Yoshihara and Ohta, 1998). The preparations used to demonstrate the conversion of milacemide to glycine by MAO-B were enriched in mitochondria (Janssens de Varebeke et al., 1988). Formation of M12 is not due to the semicarbazide-sensitive amine oxidase because the reaction is sensitive to selegiline and bicifadine is not a primary amine (Kinemuchi et al, 2004). Nonetheless, others have reported significant MAO activity in the microsomal fraction. For example, Salva et al. (2003) found almotriptan metabolism by MAO in both the microsomal and mitochondrial fractions of human liver. Yu et al. (2003) documented MAO activity for the formation of tryptophol from tryptamine in human liver microsomes. Gomez et al. (1988) demonstrated the presence of MAO-A and MAO-B activity in rat liver microsomes using enzyme-specific substrates and inhibitors and changes in temperature- and pH-sensitivity that were similar to those in mitochrondria. Iwasa et al. (2003) found that MAO activity for the metabolism of rizatriptan was similar between the microsomal and mitochondrial fractions of Japanese liver donors. In the present study, microsomal MAO activity appears to be qualitatively similar to that in the mitochondrial preparation. However, unlike other examples of microsomal MAO activity, the formation of M12 from bicifadine is a major metabolic pathway.

M12 is oxidized further to M9, mainly by mouse and monkey hepatocytes, and is a minor metabolite in rat hepatocytes; it is not detectable in human hepatocytes. The initial hydroxymethyl intermediate (M8) and its O-glucuronide (M7) were detected only in monkey hepatocyte incubations, but reaction phenotyping studies demonstrated a low capacity for M8 formation by human hepatic microsomes.

While the acid lactam, M9, can potentially be formed from M2 or M3, the results from the mouse and monkey hepatocyte incubations indicate that M12 is the more likely precursor to this metabolite. Both M12 and M8 had much higher concentrations after 1 h of incubation compared to 3 h in these two species, while M9 increased 3- to 5-fold over the same time period. These changes are indicative of a precursor-product relationship among M12, M8, and M9.

[^{14}C]Bicifadine was also metabolized to the carbamyl-O-glucuronide conjugate M11 by all four species. Similar glucuronides have been reported for tocainide (Elvin et al., 1980; Kwok et al., 1990), rimantadine (Brown et al., 1990), carvedilol (Schaefer, 1992), the benzazepine SK&F 86466 (Straub et al., 1988), and sertraline (Tremaine et al., 1989). This appears to be a minor pathway for the metabolism of bicifadine in comparison to oxidation of the methyl group and the pyrrolidine ring.

In summary, there are two main metabolic pathways of bicifadine in mouse, rat, monkey, and human microsomes and hepatocytes. One is the hydroxylation of the methyl group (via CYP2D6 in human) with subsequent oxidation to the carboxylic acid. The other is oxidation of the pyrrolidine ring, initiated by MAO-B, to form the lactam metabolite. Furthermore, it appears that lactam formation is a major metabolic route for bicifadine in microsomes, being as active as CYP for [^{14}C]bicifadine metabolism in humans.

REFERENCES

Basile AS, Janowsky A, Golembiowska K, Kowalska M, Tam E, Benveniste M, Popik P, Nikiforuk, Krawczyk M, Nowak G, Krieter PA, Lippa AS, Skolnick P, and Koustova E. (2007) Characterization of the antinociceptive actions of bicifadine in models of acute, persistent, and chronic pain. *J Pharmacol Exp Ther* **321**:1208-1225.

Beedham C (2002) Molybdenum hydroxylases, in *Enzyme Systems that Metabolise Drugs and Other Xenobiotics* (Ioannides C, ed) pp 147-187. John Wiley & Sons, New York.

Brandlange S and Lindblom L (1979) The enzyme “aldehyde oxidase” is an iminium oxidase. Reaction with nicotine delta 1’(5’) iminium ion. *Biochem Biophys Res Commun* **91**:991-996.

Brown SY, Garland WA, and Fukuda EK (1990) Isolation and characterization of an unusual glucuronide conjugate of rimantadine. *Drug Metab Dispos* **18**:546-547.

Cashman JR, Park SB, Yang ZC, Wrighton SA, Jacob P 3rd, and Benowitz NL (1992) Metabolism of nicotine by human liver microsomes: stereoselective formation of *trans*-nicotine N’-oxide. *Chem Res Toxicol* **5**:639-646.

Chiba K, Peterson LA, Castagnoli KP, Trevor AJ, and Castagnoli N (1985) Studies on the molecular mechanism of bioactivation of the selective nigrostriatal toxin 1-methyl-4-phenyl-1,2,3,6-tetrahydropyridine. *Drug Metab Dispos* **13**:342-347.

Elvin AT, Keenghan JB, Byrnes EW, Tenthorey PA, McMaster PD, Takman BH, Lalka D, Manion CV, Baer DT, Wolshin EM, Meyer MB, and Ronfeld RA (1980) Tocainide conjugation in humans: novel biotransformation pathway for primary amine. *J Pharm Sci* **69**:47-49.

Epstein JW, Osterberg AC, and Regan BA (1982) Bicifadine: nonnarcotic analgesic activity of 1-aryl-3-azabicyclo[3.1.0]hexanes. *NIDA Res Monograph* **41**:93-98.

Gomez N, Balsa N, and Unzeta M (1988) A comparative study of some kinetic and molecular properties of microsomal and mitochondrial monoamine oxidase. *Biochem Pharmacol* **37**:3407-3413.

Iwasa T, Sano H, Sugiura A, Uchiyama N, Hara K, Okochi H, Nakagawa K, Yasumori T, and Ishizaki T (2003) An *in vitro* interethnic comparison of monoamine oxidase activities between Japanese and Caucasian livers using rizatriptan, a serotonin receptor IB/ID agonist, as a model drug. *Br J Clin Pharmacol* **56:**537-544.

Janssens de Varebek P, Cavalier R, David-Remacle M, and Youdim M (1988) Formation of the neurotransmitter glycine from the anticonvulsant milacemide is mediated by brain monoamine oxidase B. *J Neurochem* **50**:1011-1016.

Kinemuchi H, Sugimoto H, Obata T, Satoh N, and Ueda S (2004) Selective inhibitors of membrane-bound semicarbazide-sensitive amine oxidase (SSAO) activity in mammalian tissues. *NeuroToxicology* **25**:325-335.

Kwok DWK, Pillai G, Vaughn R, Axelson JE, and McErlane KM (1990) Preparative HPLC and preparative TLC isolation of tocainide carbamoyl O-β-D-glucuronide: structural characterization by GC-MS and FAB-MS. *J Pharm Sci* **79**:857-861.

Obach RS (2004) Potent inhibition of human liver aldehyde oxidase by raloxifene. *Drug Metab Dispos* **32**:89-97.

Riff D, Huang N, Czobor P, and Stern W (2006) A five-day, multi-center, randomized, placebo-controlled, double-blind, efficacy and safety study of bicifadine and tramadol versus placebo in the treatment of postoperative bunionectomy pain. *J Pain* **7**(Suppl 2):S40.

Salva M, Jansat JM, Martinez-Tobed A, and Palacios J (2003) Identification of the human liver enzymes involved in the metabolism of the antimigraine agent almotriptan. *Drug Metab Dispos* **31**:404-411.

Schaefer WH (1992) Formation of a carbamoyl glucuronide conjugate of carvedilol *in vitro* using dog and rat liver microsomes. *Drug Metab Dispos* **20**:130-132.

Schnaitman C, Erwin VG, and Greenawait JW (1967) The submitochondrial localization of monoamine oxidase. An enzymatic marker for the outer membrane of rat liver mitochondria. *J Cell Biol* **32**:719-735.

Stern W, Czobor P, Stark J, and Krieter P (2005) Relationship between plasma bicifadine levels and analgesic effect in a dental pain model. Sydney, Australia. Abstracts 11th World Congress International Association for the Study of Pain, page 111.

Stern W, Pontecorvo M, Czobor P, Waldron D, and Apfel S (2006) A multi-center, randomized, active comparator-controlled study to evaluate the long-term safety and efficacy of bicifadine for the treatment of chronic low back pain (CLBP). *J. Pain* **7** (Suppl 2): S40.

Straub K, Davis M and Hwang B (1988) Benzazepine metabolism revisited: evidence for the formation of novel amine conjugates. *Drug Metab Dispos* **16:**359-366.

Tremaine LM, Stroh JG, and Ronfeld RA (1989) Characterization of a carbamic acid ester glucuronide of the secondary amine sertraline. *Drug Metab Dispos* **17:**58-63.

Vickers S and Polsky SL (2000) The biotransformation of nitrogen containing xenobiotics to lactams. *Cur Drug Metab* **1:**357-389.

Yoshihara S and Ohta S (1998) Involvement of hepatic aldehyde oxidase in conversion of 1-methyl-4-phenyl-2,3-dihydropyridinium ($MPDP^+$) to 1-methyl-4-phenyl-5,6-dihydro-2-pyridone *Arch Biochem Biophysics* **360**:93-98.

Yu A-M, Granvil CP, Haining RL, Krausz KW, Corchero J, Küpfer A, Idle JR, and Gonzalez FJ (2003) The relative contribution of monoamine oxidase and cytochrome P450 isozymes to the metabolic deamination of the trace amine tryptamine. *J Pharmacol Exp Ther* **304:**539-546.

Footnote

Address correspondence to: Dr. Philip Krieter, DOV Pharmaceutical, 150 Pierce Street, Somerset, NJ 08873. E-mail: pkrieter@dovpharm.com.

Figure Legends

Fig 1. Structure of Bicifadine HCl. The asterick marks the position of the [^{14}C]radiolabel.

Fig 2. Radioflow HPLC analysis of [^{14}C]bicifadine metabolites generated by hepatic microsomes from the mouse, rat, monkey, and human. [^{14}C]Bicifadine (10 μM) was incubated with hepatic microsomes for 30 min at 37°C and the suspensions were extracted and analyzed as outlined in *Materials and Methods*.

Fig 3. Radioflow HPLC analysis of [^{14}C]bicifadine metabolites generated by isolated hepatocytes from the mouse, rat, monkey, and human. [^{14}C]Bicifadine (10 μM) was incubated with isolated hepatocytes for 180 min at 37°C and the suspensions were extracted and analyzed as outlined in *Materials and Methods*.

Fig 4. Product ion mass spectra of [^{14}C]bicifadine (*m/z* 176) (a) and product ion mass spectrum of [^{14}C]M12 (*m/z* 190) from the mouse hepatocyte sample incubated for 60 min with 10 μM [^{14}C]bicifadine (b). The asterisk indicates the position of the [^{14}C]label in the molecule.

Fig 5. Proposed biotransformation pathways of [^{14}C]bicifadine in the mouse, rat, monkey, and human. The asterisk indicates the position of the radiolabel in [^{14}C]bicifadine.

Fig 6. Radioflow HPLC analysis of [^{14}C]bicifadine metabolites generated by human hepatic microsomes incubated for 30 min with 1 μM [^{14}C]bicifadine with (top) and without (bottom) NADPH.

Fig 7. Effect of CYP450-selective inhibitors on the rate of formation of M2 by human hepatic microsomes incubated with 1 μM [^{14}C]bicifadine. The specific inhibitors were 10 μM α-napthoflavone (CYP1A2), 5 μM sulfaphenazole (CYP2C9), 25 μM omeprazole (CYP2C19), 10 μM quinidine (CYP2D6), 100 μM DETC (CYP2E1), and 1 μM ketoconazole (CYP3A4). After 30 min of incubation, the suspensions were extracted and analyzed by radioflow HPLC as detailed in *Materials and Methods*. CYP2C19 activity is the average of 2 incubations rather than a mean (SD) of 3 incubations as for the other reactions.

Fig 8. Michaelis-Menten plot of the formation of M12 from [^{14}C]bicifadine by human hepatic microsomes in the absence of NADPH.

Fig 9. The effect of the aldehyde oxidase inhibitor perphenazine on the formation of bicifadine lactam M12 and the AO substrate phthalazone in cytosol, microsomes, and mitochondria. The concentrations of phthalazine and

perphenazine were 10 μM and 1 μM, respectively. The control activities of AO (pmol of phthalazinone/min/mg protein) were 42.4, 20.2 and 376 in the microsomes, mitochondria, and cytosol, respectively. Formation of M12 using liver cytosol was not determined.

DMD Fast Forward. Published on September 19, 2007 as DOI: 10.1124/dmd.107.016055
This article has not been copyedited and formatted. The final version may differ from this version.

TABLE 1

Metabolism of [^{14}C]Bicifadine by Mouse, Rat, Monkey, and Human Hepatic Microsomes

Microsomes were incubated with 10 μM [^{14}C]bicifadine for 30 min with and without NADPH as described in *Materials and Methods*. The formation of the products was measured using HPLC with radioflow detection.

Species	NADPH	M2	M3	M8	Bicifadine	M12
Mouse	+ NADPH	2.4	N.D.	N.D.	68.3	18.1
	- NADPH	N.D.	N.D.	N.D.	75.8	16.8
Rat	+ NADPH	5.0	ND	ND	68.8	7.8
	- NADPH	N.D.	0.7	ND	74.4	4.9
Monkey	+ NADPH	7.5	0.9	1.6	44.7	36.2
	- NADPH	N.D.	0.7	ND	54.1	36.3
Human	+ NADPH	6.2	N.D.	N.D.	71.7	6.0
	- NADPH	N.D.	N.D.	N.D.	84.4	7.1

N.D. Not detected by radioflow detector

TABLE 2

Metabolism of [^{14}C]Bicifadine by Mouse, Rat, Monkey, and Human Hepatic Hepatocytes

Isolated hepatocytes (0.75 x 10^6 cells/ml) were incubated with 10 μM [^{14}C]bicifadine with an atmosphere of 5% CO_2 at 37°C for 60 and 180 min as described in *Materials and Methods*. The formation of the products was measured using HPLC with radioflow detection.

Species	Time	M1	M2	M3	M4	M5	M6	M7	M8	M9/M10[a]	Bicifadine[a]	M11	M12
Mouse	0 min	ND	ND	ND	ND	ND	ND	ND	ND	ND	96.6	ND	ND
	60 min	0.34	6.6	10.5	ND	ND	ND	ND	2.7	M9 7.3	22.7	4.4	44.2
	180 min	1.2	1.2	25.0	ND	ND	ND	ND	0.5	M9 35.9	9.9	5.9	16.7
Rat	0 min	ND	0.6	0.7	ND	ND	ND	ND	ND	ND	91.1	ND	ND
	60 min	Y	2.5	7.8	ND	Y	Y	ND	ND	M10 2.3	44.8	3.8	30.5
	180 min	Y	1.2	13.3	ND	1.2	Y	ND	ND	M9/10 4.2	13.2	4.7	56.2
Monkey	0 min	ND	ND	ND	ND	ND	ND	ND	ND	ND	95.9	ND	ND
	60 min	0.4	29.0	14.1	1.9	ND	ND	1.2	20.1	M9 8.9	6.3	1.3	17.9
	180 min	1.6	17.9	24.4	1.9	ND	ND	5.9	8.5	M9 29.5	3.6	1.5	Y
Human	0 min	ND	ND	ND	ND	ND	ND	ND	ND	ND	96.7	ND	ND
	60 min	Y	2.7	5.9	ND	Y	Y	ND	ND	M10 5.1	26.8	2.7	55.6
	180 min	Y	1.5	13.2	ND	Y	Y	ND	ND	M10 7.8	6.5	2.5	66.4

ND Not detected

Y Detected by LC/MS/MS but <0.3% of profiled radioactivity

a: Percentages of bicifadine, M9, and M10 at 60 and 180 min derived from LC/MS/MS sample runs.

TABLE 3

Major CID Product Ions of Metabolites of [^{14}C]Bicifadine

Metabolite	M + H^+	Major CID Fragment Ions (*m/z*)
Bicifadine	174	157 (-NH_3), 142, 133 (base peak, -C_2H_3N), 129, 118, 105 (*m/z* 133 - C_2H_4), 91 (tropylium ion), 82
DOV 255,833 (M9)	218	201 (-NH_3), 200 (-H_2O), 182, 171, 164, 146, 135 (base peak), 129, 118, 107, 96, 91, 83, 55
DOV 255,838 (M12)	188	171 (-NH_3), 170 (-H_2O), 143, 134, 105 (base peak), 96, 55
[^{14}C]Bicifadine	176	159 (-NH_3), 144, 133 (base peak, -C_2H_3N), 131, 118, 105 (*m/z* 133 - C_2H_4), 91 (tropylium ion), 84
[^{14}C]M1	368	192 (-glucuronic acid), 174 (base peak, *m/z* 192-H_2O), 157 (*m/z* 174 - NH_3), 143, 113, 105, 84
[^{14}C]M2	192	175 (-NH_3), 162, 157, 149 (base peak, -C_3H_3N), 145 (*m/z* 175 - C_2H_6), 130, 121 (*m/z* 149-C_2H_4)
[^{14}C]M3	206	189 (-NH_3), 171, 163 (base peak, -C_2H_3N), 145 (*m/z* 189 - CO_2), 135 (*m/z* 163 - C_2H_4), 130, 128, 117
[^{14}C]M4	481	463 (-H_2O), 352 (-glutamic acid), 174 (base peak, -glutathione)
[^{14}C]M5	262	244 (-H_2O), 220 (-acetyl), 204 (base peak), 202, 186, 163, 146, 135, 99
[^{14}C]M6	262	220 (-acetyl), 204 (base peak), 202, 186, 146, 135, 99
[^{14}C]M7	382	206 (-glucuronic acid), 188 (base peak, *m/z* 206 - H_2O), 159, 143, 133, 115
[^{14}C]M8	206	188 (-H_2O), 174, 159 (base peak, -$^{14}CH_3NO$), 150, 129, 121, 105, 93, 84, 57
[^{14}C]M9	220	203 (-NH_3), 202 (-H_2O), 184, 173, 164, 159, 146, 135 (base peak), 129, 117, 107, 98, 91, 85, 57
[^{14}C]M10	192	174 (-H_2O), 146, 134 (base peak, -C_3H_4O), 131, 117, 105, 91 (tropylium), 74, 59
[^{14}C]M11	396	220 (base peak, -glucuronic acid), 176, 159, 132, 105, 85, 71
[^{14}C]M12	190	173 (-NH_3), 172 (-H_2O), 143, 134, 105 (base peak), 98, 57

DMD Fast Forward. Published on September 19, 2007 as DOI: 10.1124/dmd.107.016055
This article has not been copyedited and formatted. The final version may differ from this version.

TABLE 4

Effect of Clorgyline and Selegiline on the Metabolism of [^{14}C]Bicifadine to M2 by Human Liver Microsomes and Mitochondrial Preparations

Pooled human liver microsomes (0.5 mg/ml) and mitochondria (1 mg/ml) were incubated with increasing concentrations of clorgyline or selegiline for 37°C for 20 min. [^{14}C]Bicifadine (1 μM) was then added and the incubation continued for an additional 30 min. The incubations were assayed for metabolites as detailed in *Materials and Methods*.

		Activity ± SD (pmol/min/mg protein)	
	Concentration (μM)	Microsomes	Mitochondria
Control	0.0	37.7 ± 1.1	17.3 ± 0.06
Selegiline	0.001	40.2 ± 1.9	13.9 ± 3.2
	0.01	37.1 ± 3.2	14.6 ± 2.9
	0.1	4.30 ± 0.95	3.56 ± 0.41
	1	2.35 ± 0.05	2.67 ± 0.30
Clorgyline	0.001	40.5 ± 1.7	15.8 ± 1.5
	0.01	38.9 ± 1.3	17.8 ± 1.1
	0.1	36.3 ± 0.3	14.4 ± 0.3
	1	33.6 ± 0.5	14.0 ± 0.5

DMD Fast Forward. Published on September 19, 2007 as DOI: 10.1124/dmd.107.016055
This article has not been copyedited and formatted. The final version may differ from this version.

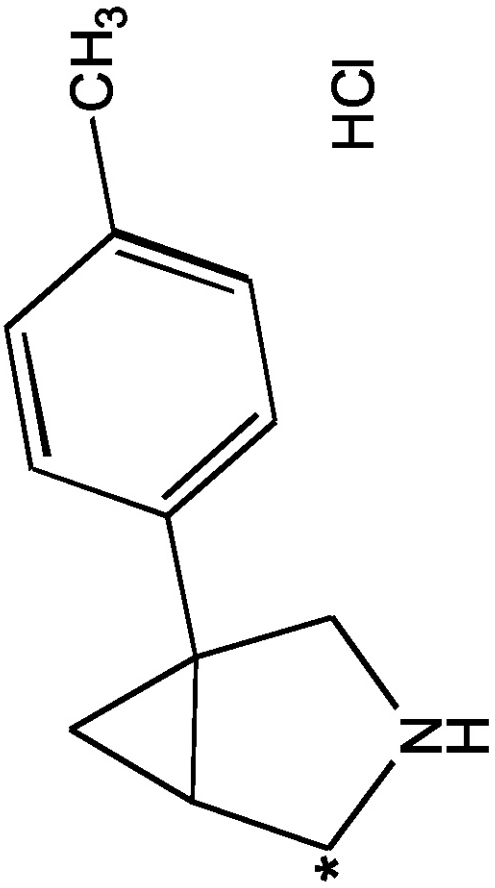

Figure 1

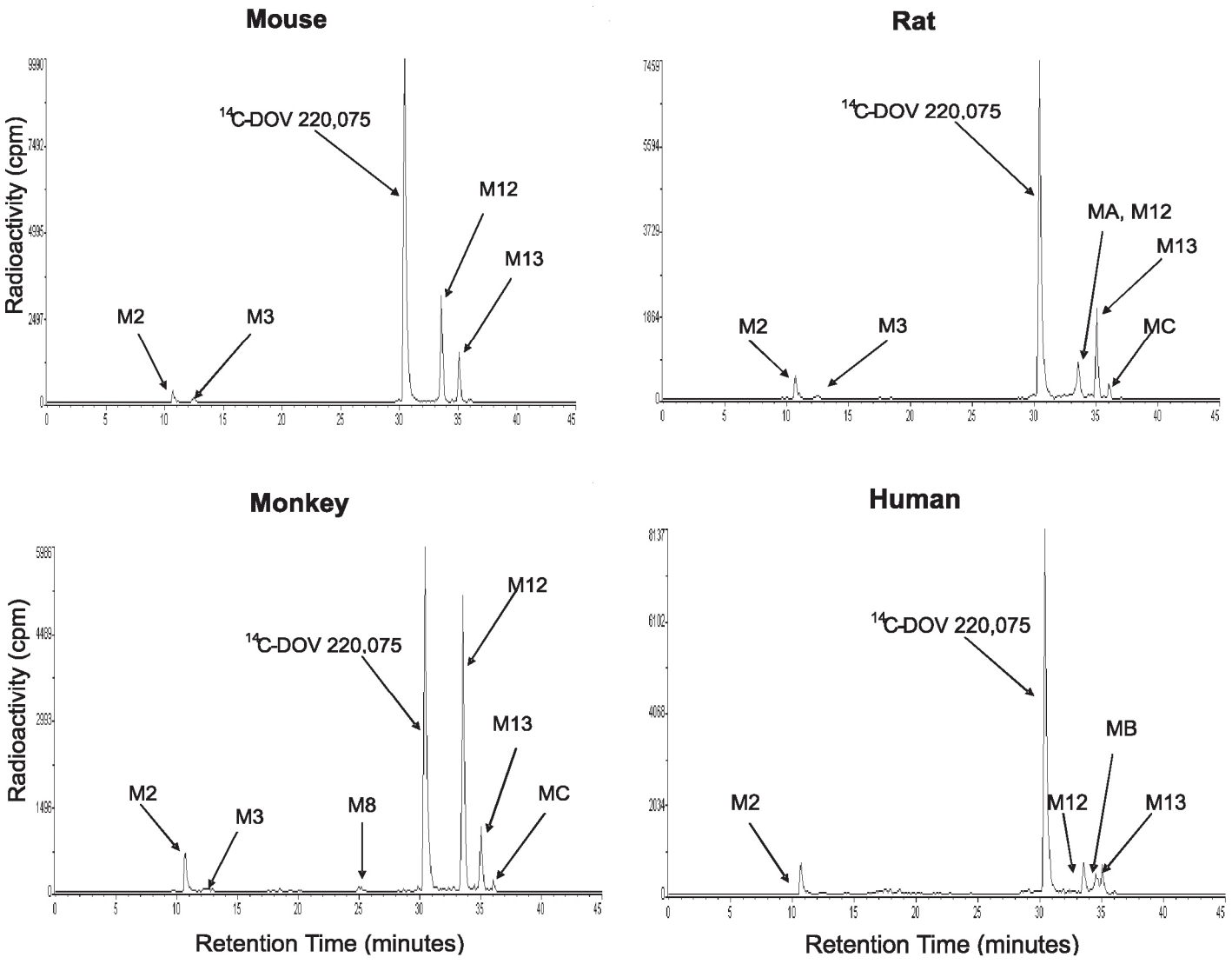

Figure 2

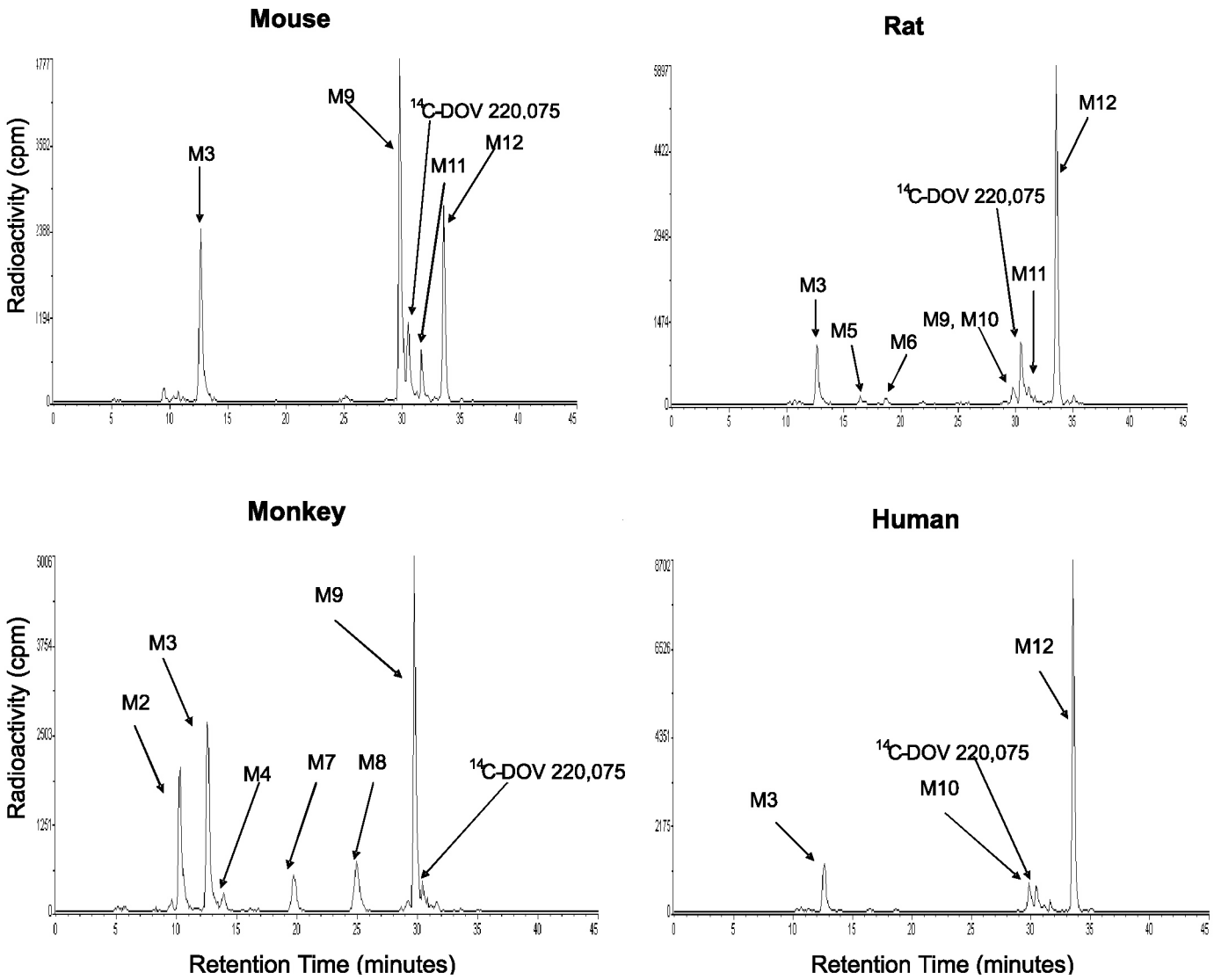

Figure 3

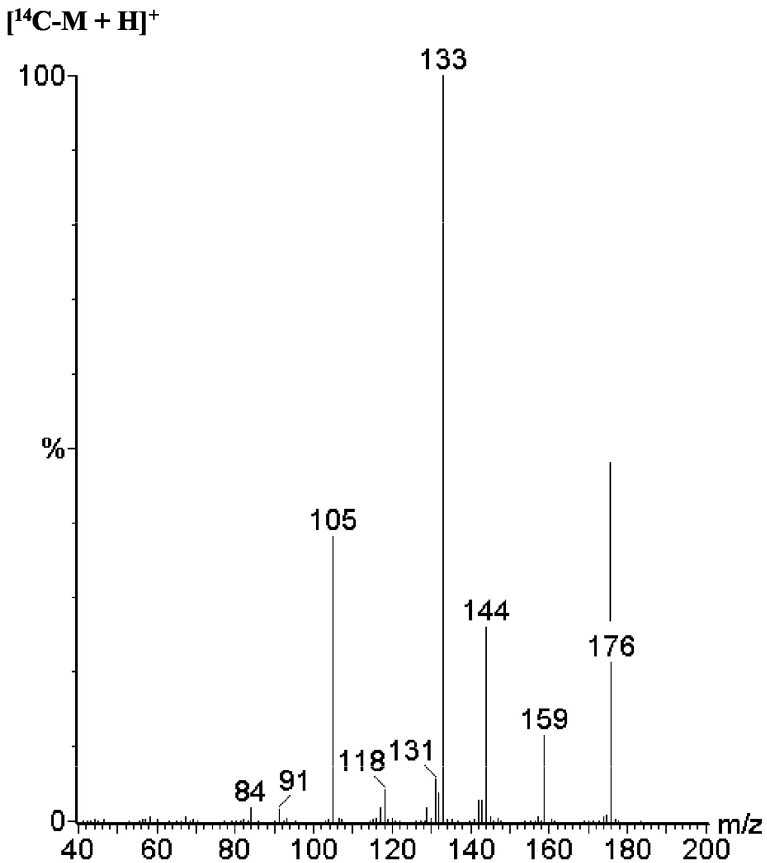

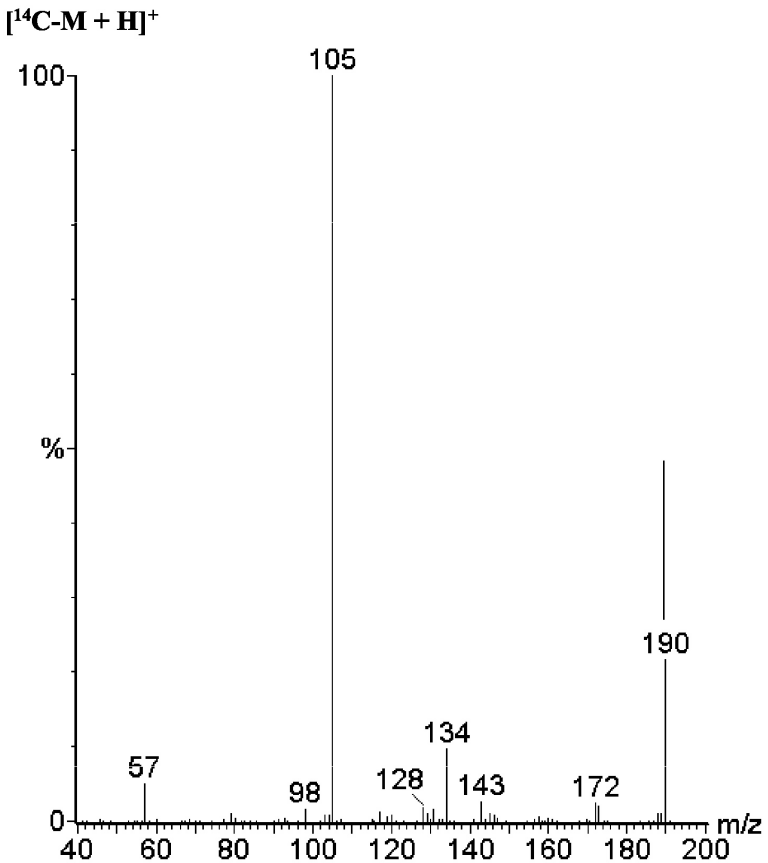

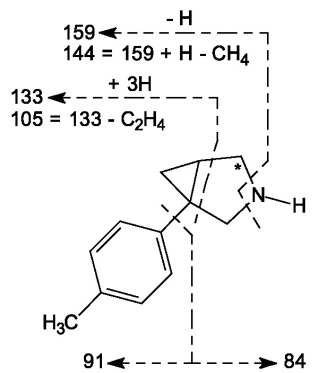

Figure 4

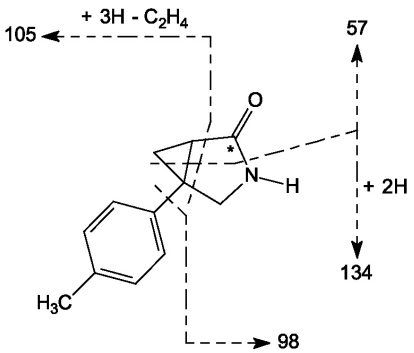

DMD Fast Forward. Published on September 19, 2007 as DOI: 10.1124/dmd.107.016055

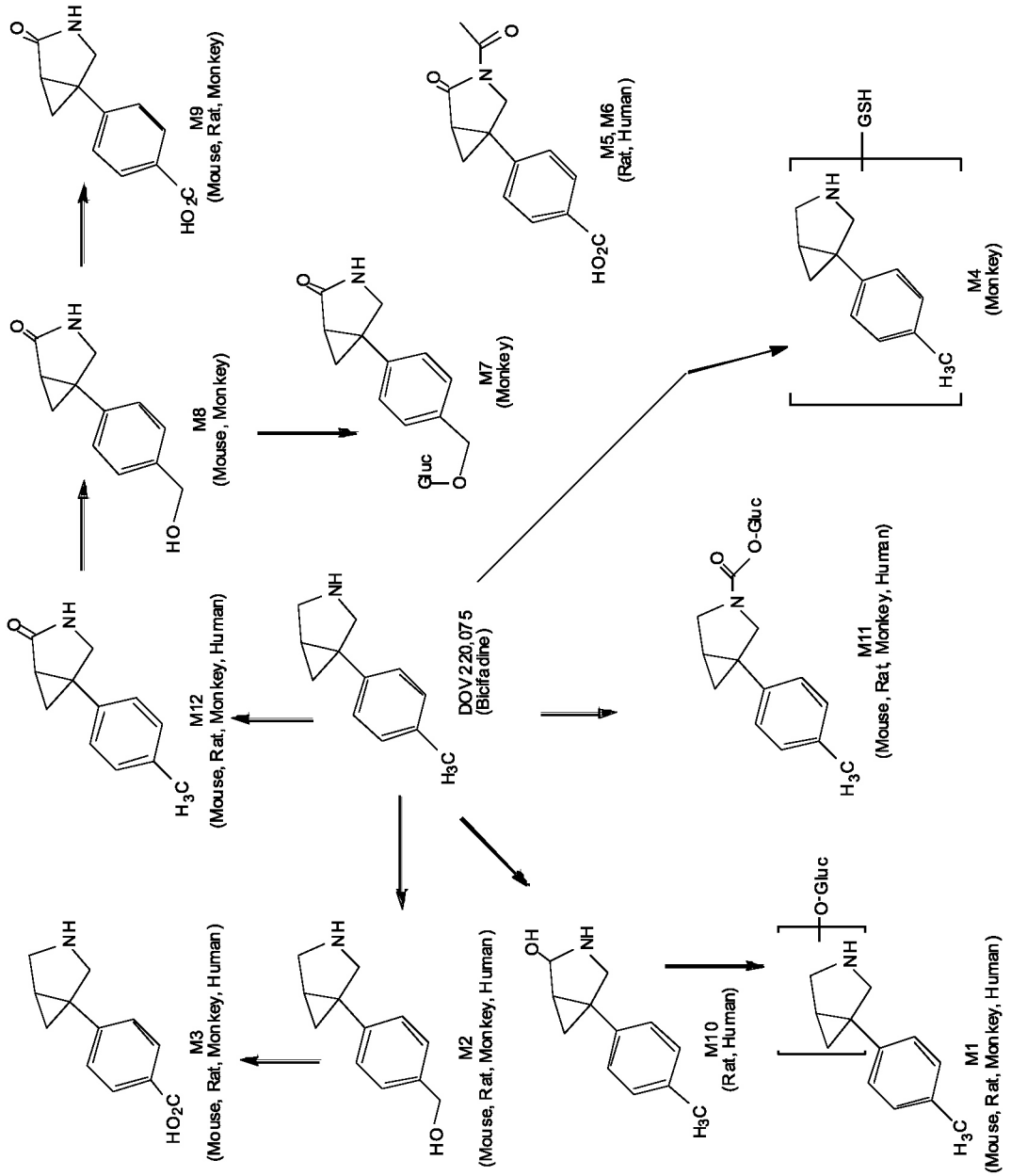

Figure 5

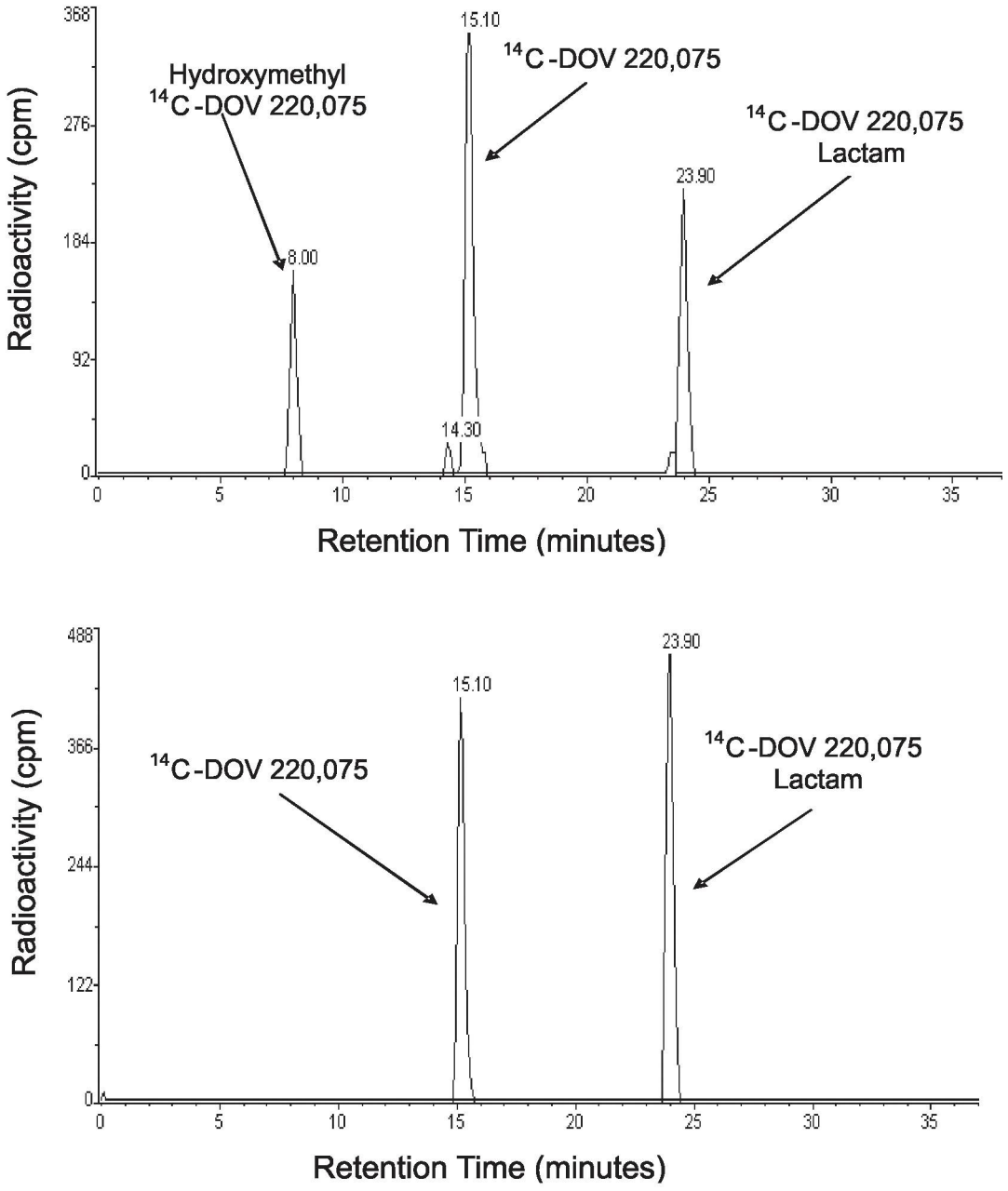

Figure 6

DMD Fast Forward. Published on September 19, 2007 as DOI: 10.1124/dmd.107.016055
This article has not been copyedited and formatted. The final version may differ from this version.

DMD Fast Forward. Published on September 19, 2007 as DOI: 10.1124/dmd.107.016055
This article has not been copyedited and formatted. The final version may differ from this version.

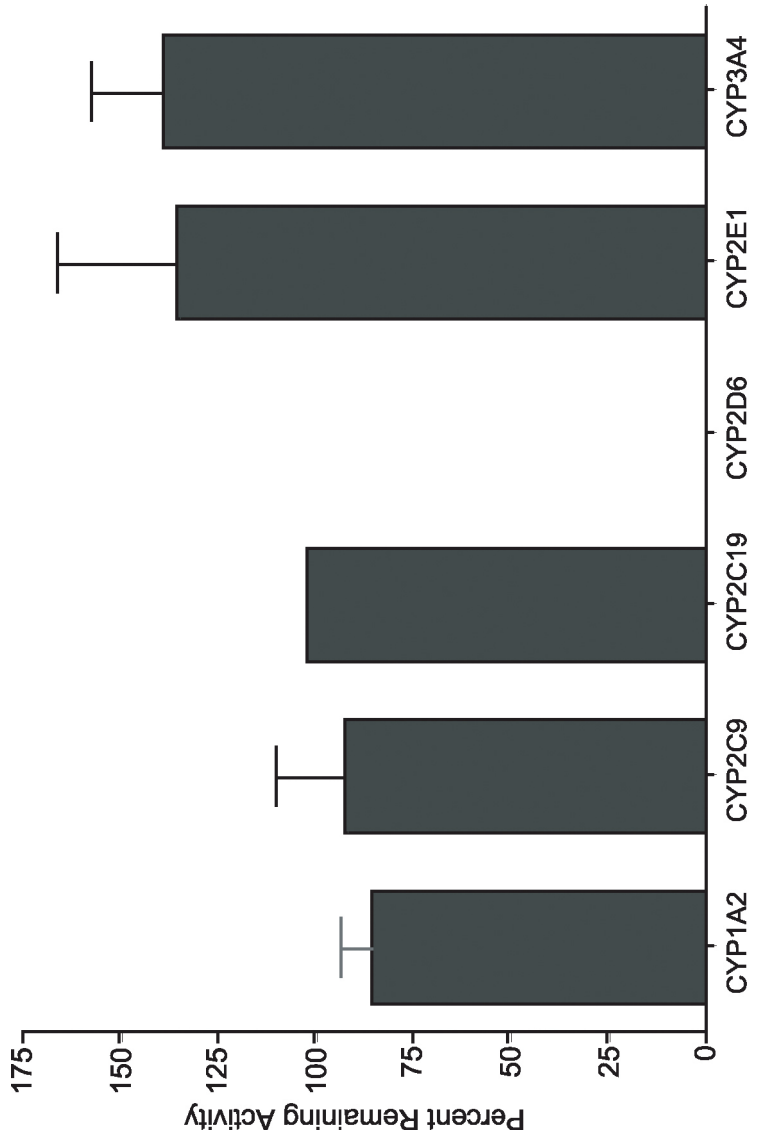

Figure 7

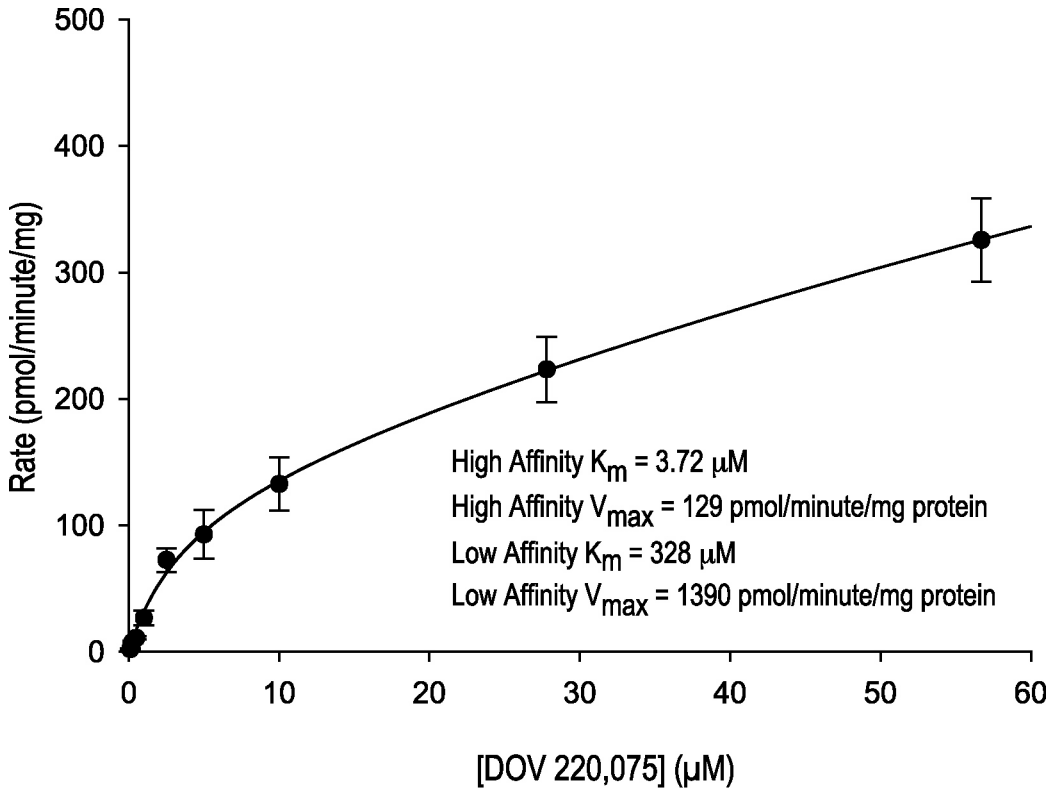

Figure 8

DMD Fast Forward. Published on September 19, 2007 as DOI: 10.1124/dmd.107.016055
This article has not been copyedited and formatted. The final version may differ from this version.

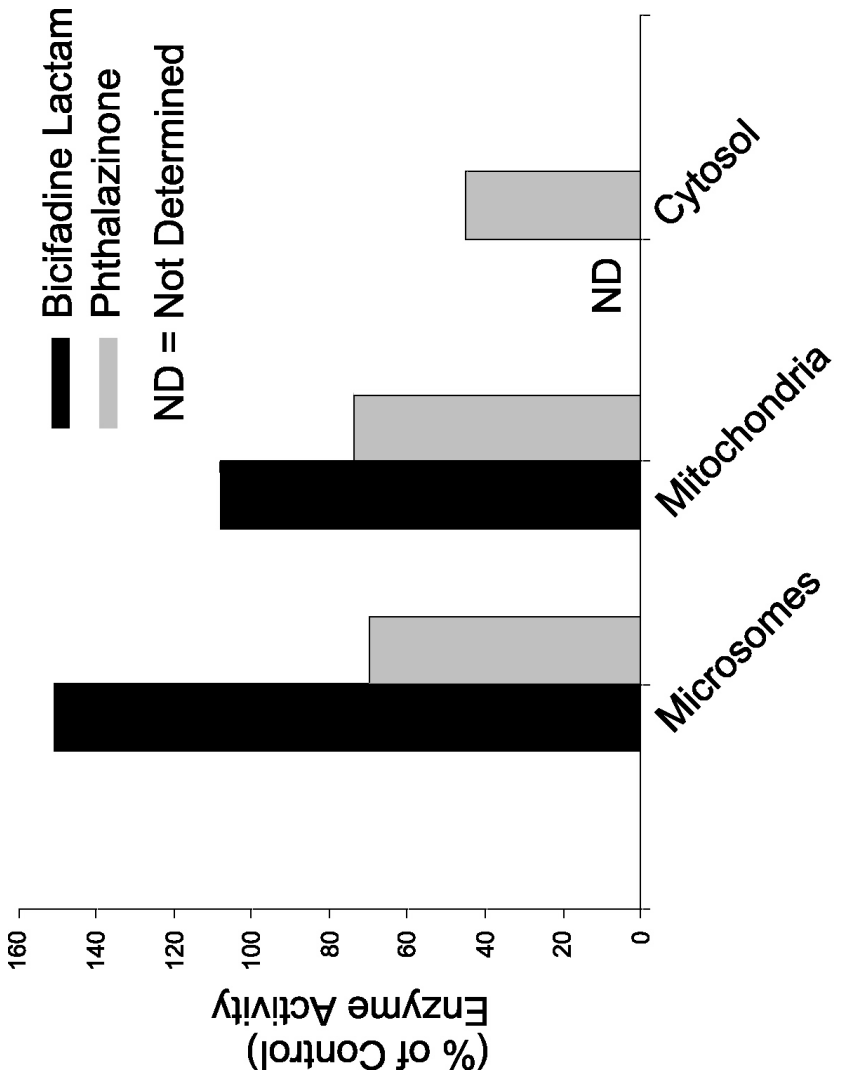

Figure 9